Journal of Medicinal Chemistry

Article

pubs.acs.org/jmc

Small Molecule STAT5-SH2 Domain Inhibitors Exhibit Potent Antileukemia Activity

Brent D. G. Page,[†,∥] Haytham Khoury,[‡,∥] Rob C. Laister,[‡] Steven Fletcher,[†] Megan Vellozo,[‡] Alessia Manzoli,[‡] Peibin Yue,[§] James Turkson,[§] Mark D. Minden,*[,‡] and Patrick T. Gunning*[,†]

[†]Department of Chemistry, University of Toronto, 3359 Mississauga Road North, Mississauga, ON, L5L 1C6, Canada

[‡]Princess Margaret Hospital, Ontario Cancer Institute, 610 University Avenue, Toronto, ON M5G 2M9, Canada

[§]Department of Molecular Biology and Microbiology, Burnett College of Biomedical Sciences, University of Central Florida, Orlando, Florida 32826, United States

Supporting Information

ABSTRACT: A growing body of evidence shows that Signal Transducer and Activator of Transcription 5 (STAT5) protein, a key member of the STAT family of signaling proteins, plays a pivotal role in the progression of many human cancers, including acute myeloid leukemia and prostate cancer. Unlike STAT3, where significant medicinal effort has been expended to identify potent direct inhibitors, Stat5 has been poorly investigated as a molecular therapeutic target. Thus, in an effort to identify direct inhibitors of STAT5 protein, we conducted an *in vitro* screen of a focused library of SH2 domain binding salicylic acid-containing inhibitors (∼150) against STAT5, as well as against STAT3 and STAT1 proteins for SH2 domain selectivity. We herein report the identification of several potent (K_i < 5 μM) and STAT5 selective (>3-fold specificity for STAT5 cf. STAT1 and STAT3) inhibitors, **BP-1-107**, **BP-1-108**, **SF-1-087**, and **SF-1-088**. Lead agents, evaluated in K562 and MV-4-11 human leukemia cells, showed potent induction of apoptosis (IC_{50}'s ∼ 20 μM) which correlated with potent and selective suppression of STAT5 phosphorylation, as well as inhibition of STAT5 target genes *cyclin D1*, *cyclin D2*, *C-MYC*, and *MCL-1*. Moreover, lead agent **BP-1-108** showed negligible cytotoxic effects in normal bone marrow cells not expressing activated STAT5 protein. Inhibitors identified in this study represent some of the most potent direct small molecule, nonphosphorylated inhibitors of STAT5 to date.

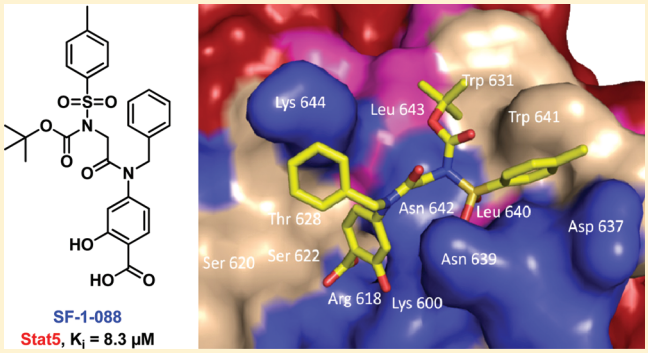

INTRODUCTION

The Signal Transducers and Activators of Transcripion (STAT) family of proteins play important and diverse cell signaling and transcriptional roles in cells. STAT signaling is transiently activated in normal cells and is deactivated by a number of different cytosolic and nuclear regulators, including phosphatases, SOCS, PIAS, and proteasomal degradation.[1] Of the seven STAT isoforms (STAT1, STAT2, STAT3, STAT4, STAT5a, STAT5b, and STAT6), STAT3 and STAT5 have gained notoriety for their aberrant role in human cancers and tumorigenesis.[2] Abnormal STAT5 activity has been found in many cancers, including those of the breast, liver, prostate, blood, skin, head, and neck.[2] Because of their similar structures and function (93% sequence homology),[2] we will use the term STAT5 to mean both STAT5a and STAT5b and will use the specific notation of STAT5a or STAT5b when referring to a specific isoform of the STAT5 protein. Despite significant evidence implicating STAT5's causal role in human malignancies, there has been very little progress in identifying small molecule inhibitors of STAT5 function. The majority of medicinal research on STAT function in transformed cells has been aimed at identifying an inhibitor of STAT3 protein. As a result, several direct inhibitors of STAT3 including peptidomimetics, small molecules, and oligonucleotide-based inhibitors have entered preclinical trials as a STAT3-targeting therapeutic.[3−5] Progress toward a potent and direct inhibitor of STAT5 function for the treatment of human malignancies has been disappointingly limited.

STAT5 activation involves a complex signaling cascade beginning at the cell surface. Stimulation by growth factors such as Kit ligand/Stem Cell Factor, erythropoietin, or prolactin results in receptor dimerization and activation of STAT5 by intracellular kinases such as Janus Kinases (JAKs).[6] In addition, oncogenes such as BCR-ABL and FLT3-ITD induce activation of STAT5. Phosphorylation of the receptor's cytoplasmic tail provides docking sites for recruitment of monomeric, nonphosphorylated STAT5 proteins via their SH2 domain. Activated tyrosine kinases, such as JAK2 phosphorylate recruited STAT5 proteins at a specific tyrosine near the

Received: June 6, 2011
Published: December 9, 2011

dx.doi.org/10.1021/jm200720n | J. Med. Chem. 2012, 55, 1047−1055

Table 1. Comparative STAT Isoform Selectivity Data (K_i Values, μM) as Assessed by STAT5, STAT3 and STAT1 FP Assays

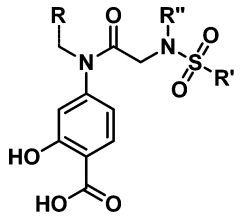

	R	R'	R''	Stat5b	Stat3	Stat1
SF-1-066	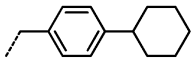	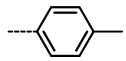	—CH_3	> 25	15.5 ± 4.7	> 25
BP-1-075	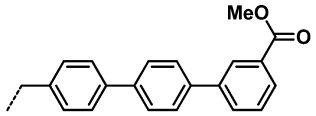	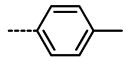	—CH_3	3.8 ± 1.6	2.8 ± 1.1	3.2 ± 1.3
BP-2-122	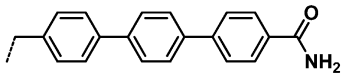	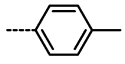	—CH_3	4.8 ± 1.6	8.4 ± 2.4	9.5 ± 2.4
SF-2-096	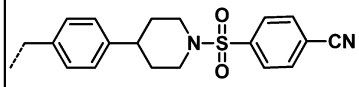	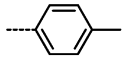	—CH_3	7.3 ± 0.9	8.4 ± 0.9	> 25
SF-3-006	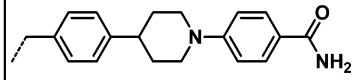	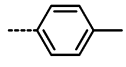	—CH_3	10.1 ± 1.5	17.6 ± 0.8	27.8 ± 2.2
BP-1-107	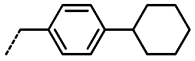	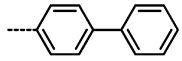	—CH_3	4.1 ± 0.5	6.2 ± 2.0	8.8 ± 1.6
BP-1-108	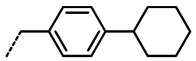	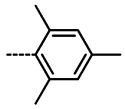	—CH_3	2.8 ± 3.2	8.0 ± 2.4	9.7 ± 8.2
BP-1-111	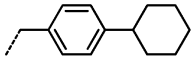	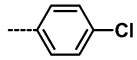	—CH_3	7.9 ± 2.1	11.0 ± 0.2	22.0 ± 3.9
SF-1-087	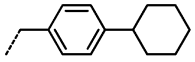	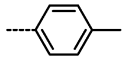	—Boc	3.4 ± 0.9	7.9 ± 0.1	> 25
SF-1-088	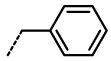	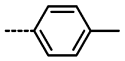	—Boc	8.3 ± 6.1	> 25	> 25

carboxy terminus (Tyr694 in STAT5a and Tyr699 in STAT5b). Phosphorylated STAT5 (pSTAT5) protein is released from the receptor, and dimerization occurs through reciprocal phosphotyrosine−SH2 domain interactions. Phosphorylation of a serine residue then allows the STAT5 dimers to translocate to the nucleus where STAT5 binds to a consensus DNA sequence and promotes gene expression.[2,7]

In cancer cells, STAT5 is routinely constitutively phosphorylated which leads to the aberrant expression of STAT5 target genes resulting in malignant transformation. Cancer cells harboring persistently activated STAT5 overexpress antiapoptotic proteins such as BCL-XL, MYC, and MCL-1, conferring significant resistance to natural apoptotic cues and administered chemotherapeutic agents.[8] Of particular interest, STAT5 has been identified as a key regulator in the development and progression of acute myelogenic (AML) and acute lymphoblastic leukemias (ALL).[9−11] Moreover, inhibitors of upstream STAT5 activators (such as JAK and FLT3) have been shown to exhibit promising anticancer properties.[12,13] However, a shortcoming of tyrosine kinase inhibitors, and other upstream effectors of kinase activity, is the disruption of multiple downstream signaling pathways, increasing the likelihood of undesirable toxicity. In addition, it is possible that other proteins in the malignant cell may also be activating STAT5; this signaling would not be affected by an upstream-targeted inhibitor. Therefore, silencing a downstream signaling target such as STAT5 would ultimately result in fewer side effects and would thus represent a more attractive candidate for a molecularly targeted drug for the treatment of human cancers harboring aberrant STAT5 activity.

To date, inhibition of STAT function has been achieved through *N*-terminal domain binders, DNA binding domain-targeting oligonucleotides, and most popularly, SH2 domain binders that block STAT phosphorylation, dimerization, and target gene expression.[3−5] However, the vast majority of medicinal chemistry effort has been conducted against STAT3 and not against STAT5. To the best of our knowledge, only one family of chromone-based STAT5 SH2 domain binding small molecules has been identified as being direct inhibitors of STAT5 activity *in vitro*.[2] In this work, Berg and co-workers

dx.doi.org/10.1021/jm200720n | J. Med. Chem. 2012, 55, 1047−1055

identified several small molecule chromone-based compounds that potently bound to STAT5's SH2 domain, as assessed by a competitive STAT5 fluorescence polarization (FP) assay and by *in silico* docking studies.[14] However, despite promising *in vitro* disruption of STAT5/phosphopeptide interactions (IC_{50} ~15−50 μM), much higher concentrations of inhibitor were required to elicit the inhibition of STAT5 activation in lymphoma whole cells (100−200 μM).[2] Thus, while STAT5 remains a highly appealing and validated molecular target, the discovery of a potent STAT5 inhibitor with *in vivo* efficacy has yet to be achieved.

Thus, in an effort to identify potent and direct inhibitors of STAT5 function, we have investigated the application of small molecule scaffolds targeting STAT5's SH2 domain to disrupt STAT5 signaling and the expression of STAT5 gene targets. Through an *in silico* screening of a National Cancer Institute library of compounds, we identified compounds containing salicylic acid as being effective SH2 domain binders, likely a result of effective phosphotyrosine mimicry.[15] *In silico* docking with GOLD software showed the salicylic component making binding interactions with the key pTyr binding pocket. Upon the basis of the salicylic acid moiety, we constructed a library of rationally designed SH2 domain binders targeting STAT3's SH2 domain.[16,17] As previously reported, this SAR study yielded a number of potent STAT3 inhibitors, including **SF-1-066**,[16,17] which was shown to potently inhibit STAT3 function *in vitro* and in *in vivo* models of breast cancer.[17] Given that each inhibitor in the family possessed an SH2 binding salicylic moiety, we reasoned that our library of privileged structures could contain potent STAT5 binding agents. Thus, we screened our library of ~150 compounds for *in vitro* STAT5 SH2 domain binding activity.

RESULTS

The library was subjected to a high-throughput STAT5b FP assay to determine binding affinity for the STAT5b SH2 domain.[14] This competitive assay is based upon the small molecule-mediated displacement of a STAT5-SH2 domain binding 5-carboxyfluorescein-labeled (F*) erythropoietin phosphopeptide, F*-GpYLVLDKW from the STAT5b-SH2 domain, wherein the unbound F*-GpYLVLDKW results in reduced polarization of the emitted fluorescence due to a higher mobility of the unbound phosphopeptide fluorophore. The library was first screened for activity against STAT5b at 25 and 50 μM, and compounds eliciting potent activity at <25 μM were further evaluated to determine K_i values and STAT specificity. The most potent STAT5b inhibitors identified were subjected to previously described STAT1[18] and STAT3[19] FP assays. The STAT5, STAT3, and STAT1 K_i values are reported in Table 1.

First, as a negative control, we evaluated **SF-1-066**,[16] a previously reported, potent and selective STAT3 protein inhibitor. Unsurprisingly, **SF-1-066** showed no inhibitory effect against STAT5b or STAT1 phosphopeptide binding (K_i's > 25 μM). More generally, and most encouragingly, out of the approximately 150 compounds screened in parallel, we identified a number of lead compounds including, **BP-1-075**, **BP-1-122**, **SF-2-096**, **BP-1-107**, **BP-1-108**, **BP-1-111**, **BP-1-122**, **SF-1-087**, and **SF-1-088** that showed impressive STAT5b binding affinity (K_i's < 10 μM). Next, lead compounds were subjected to FP binding assays for both STAT3 and STAT1 affinity (Table 1., and Supporting Information). Encouragingly, of the 10 lead compounds, six agents, **BP-1-107**, **BP-1-108**, **SF-1-087**, **BP-1-111**, and **SF-1-088** showed promising STAT5b specificity (2−3-fold specificity). Most notably, **BP-1-108**, **SF-1-088**, and **BP-1-111** exhibited the highest selectivity for STAT5b (~3-fold specificity for STAT5 cf. STAT1 and STAT3). While **BP-1-075**, incorporating a large substituted terphenyl R group, was a potent binder of STAT5b (K_i = 3.8 μM), we determined that it was equipotent against both STAT1 (K_i = 3.2 μM), a tumor suppressor gene,[20] and STAT3 (K_i = 2.8 μM). Moreover, the structurally similar **BP-2-122**, showed similar STAT5b potency (K_i = 4.8 μM) as well as limited STAT isoform selectivity (<2 fold). Structurally, STAT5b inhibitors generally contained a bulky and, in most cases, hydrophobic R substituent (cyclohexylbenzyl, terphenyl or a substituted benzyl piperidyl). However, of note, **SF-1-088**, incorporating the smallest R and R′ substituent, an *N*-benzyl and tolyl group, respectively, exhibited the highest STAT5 specificity, i.e., STAT5b K_i = 8 μM cf. STAT1 and >25 μM cf. STAT3 >25 μM. Moreover, unlike the majority of STAT5b inhibitors identified in this screen, **SF-1-088** is equipped with a bulky R″ group (R″ = *N*-*tert*-butyloxycarbonyl). We also investigated the disruption of preformed STAT5−STAT5 dimers by electrophoretic mobility shift assay (EMSA) analysis of nuclear extracts taken from NIH3T3/hEGFR cells, harboring activated STAT5. While **BP-1-108** was shown to disrupt STAT5−STAT5 dimers with an IC_{50} of approximately 100 μM (Supporting Information), the modest potency exhibited in this assay suggested that this class of compound will only poorly disrupt activated STAT5 dimers. Instead, inhibitory function will most likely be derived from binding to the unphosphorylated STAT5 monomer and thus prevent STAT5 phosphorylation and/or binding to the phosphorylated STAT5 protein disrupting the formation of STAT5 dimers.

Next, computational docking analysis using Genetically Optimized Ligand Docking Software (GOLD)[21] of agents was performed with the STAT5a crystal structure (pdb:1Y1U[6]). Given the near identical sequences of the STAT5a and STAT5b SH2 domains (>93%), we reasoned that inhibitor docking in silico with the STAT5a crystal structure may also offer some insight into possible inhibitor binding to STAT5b's SH2 domain. GOLD docking studies revealed that the salicylic acid component of **SF-1-088** docks within the STAT5a pTyr binding site composed of polar residues Arg618, Lys600, and Ser622 (Figure 1). The

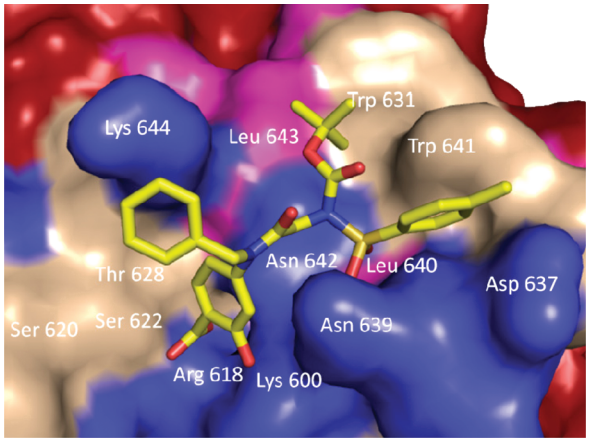

Figure 1. Low energy GOLD[45]-docked **SF-1-088** (yellow) in the STAT5a SH2 domain (pdb: 1Y1U): pink = hydrophobic residues; blue = hydrophilic residues.

dx.doi.org/10.1021/jm200720n | *J. Med. Chem.* 2012, 55, 1047−1055

hydrophobic benzyl substituent interacts with the hydrophobic portion of the Lys644 side chain as well as with the Leu643 side chain. The *tert*-butyl portion of the *N*-*tert*-butyloxycarbonyl group forms van der Waals interactions with Leu643 and Trp631. **SF-1-088**'s tetrapodal projection of functionality facilitates access to a number of subpockets within the STAT5a SH2 domain. Future work will seek to delineate inhibitor binding via a thorough structure−activity relationship against STAT5's SH2 domain.

We next assessed the whole cell potency of lead STAT5 inhibitors in the acute myeloid leukemia cell line, MV-4-11, known to harbor activated STAT5 via constitutive FLT-3 kinase activity,[22] as well as in K562 leukemia cells, which also contain constitutive STAT5 activity via the presence of BCR-ABL.[23] Both cancer cell lines were treated with inhibitors, **BP-1-107**, **BP-1-108**, **SF-1-087**, **BP-1-075**, and **SF-1-088** at 10, 20, and 40 μM concentrations and cell viabilities determined using Almar Blue (Invitrogen) fluorescent staining in 96-well plates over 3 consecutive days. Encouragingly, in MV-4-11 cells, we found that **BP-1-108**, **SF-1-087**, and **BP-1-075** inhibited cell viability with IC_{50} values of 17, 51, and 24 μM, respectively (Table 2). Similarly, in K562 cells, **BP-1-075** and **BP-1-108** inhibited cell viability with IC_{50} values of 24 and 42 μM, respectively. The cytotoxic potential of **BP-1-108** was confirmed using an Annexin V/PI assay in K562 cells. In this assay, **BP-1-108** (40 μM, 24 h) induced apoptosis in K562 cells as measured by annexin V staining (Supporting Information). In contrast, **BP-1-108** minimally affected healthy patient bone marrow cells that do not harbor constitutive STAT5 activity (Supporting Information) even at concentrations of up to 160 μM. To determine whether the biological effects correlated with intracellular STAT5 suppression, we next measured inhibitor mediated suppression of STAT5 phosphorylation in the K562 cells.

Table 2. Selected IC_{50} Values (μM) of Inhibitors in MV-4-11 and K562 Cells at 48 h Post-Treatment

	IC_{50} values (μM)	
compd	MV-4−11	K562
SF-1-088	>80	77 ± 5
SF-1-087	51 ± 7	>80
BP-1-107	>80	80 ± 18
BP-1-108	17 ± 1	42 ± 16
BP-1-075	24 ± 2	24 ± 3

To evaluate the inhibition of intracellular STAT5 in K562 leukemia cells, carrying the *BCR-ABL* oncogene, were treated with **BP-1-107**, **BP-1-108**, **SF-1-087**, and **SF-1-088**. After 6 h of exposure to the drug, we measured the level of STAT5 phosphorylation by Western blot analysis. Consistent with the cytoxic effects on leukemia cells, we observed dose-dependent inhibition of STAT5 phosphorylation after treatment with inhibitors confirming that these agents inhibit oncogene mediated STAT5 activation in tumor cells (Figure 2A and Supporting Information). Presumably, this resulted from the blockade of STAT5 binding to the pTyr motifs in BCR-ABL or other proteins recruited by BCR-ABL, and the subsequent prevention of *de novo* phosphorylation of STAT5 by tyrosine kinases. We next evaluated **BP-1-108** induced dose-dependent decreases in pSTAT5, pSTAT3, and pAKT using phospho-flow cytometry to measure inhibitor-induced effects. As shown in Figure 2B, and consistent with the Western blot studies, **BP-1-108** is a potent inhibitor of STAT5 phosphorylation. Moreover, **BP-1-108** elicited minimal perturbation of both pSTAT3 (Figure 2C) and pAKT (Figure 2D) phosphorylation in K562 cells at 40 μM, suggesting a STAT5 specific effect.

The above data suggests that the growth inhibitory effect of **BP-1-108** is as a result of blocking the phosphorylation of STAT5. Alternatively, the drug might be causing death due to the inhibition of phosphorylation of other down stream targets of BCR-ABL. Analysis by phospho-flow cytometry also indicates that **BP-1-108** does not affect the level pERK 1,2. Finally, to demonstrate that **BP-1-108** is not acting directly on the tyrosine kinase activity of BCR-ABL we compared the effect of the BCR-ABL inhibitor imatinib to **BP-1-108**. As can be seen in Figure 3, imatinib caused a marked reduction in both pSTAT5 and pERK1,2, while **BP-1-108** only blocked the phosphorylation of pSTAT5. Taken together, this suggests that **BP-1-108** does not inhibit the JAK/STAT3 pathway, the PI3K pathway, or MAPK pathways and that it specifically inhibits the phosphorylation of STAT5.

To exclude the possibility that this effect on STAT5 was a peculiarity of cells with an activated oncogene, we used the IL-3 dependent cell line 32D. The level of pSTAT5 was determined by flow cytometry. In the presence of IL-3, the peak is shifted to the left in comparison to no IL-3. The addition of **BP-1-108** to cells grown in IL-3 resulted in a major reduction in the level of pSTAT5 (shown in Figure 4).

Previous reports indicate that knockdown of phosphorylated STAT5 (pSTAT5) in AML cells abrogates MCL-1 expression at both the mRNA and protein level and is sufficient to induce apoptosis.[26] Indeed, suppression of MCL-1 in chronic lymphocytic leukemia and myeloma cells rapidly induced apoptosis, identifying MCL-1 as a potential key therapeutic target. Critically, in AML cells, MCL-1 expression is highly dependent upon STAT5 mediated signaling pathways, suggesting that STAT5 inhibitors might be important for triggering apoptosis in AMLs. Thus, we reasoned that promising inhibitors of STAT5 should decrease target gene expression, including *MCL-1*, *cyclin D1/D2*, and *BCL-XL*, and induce apoptosis as was observed in K562 and MV-4-11 viability assays. To confirm the inhibitory effects of lead STAT5 inhibitors, we conducted experiments to measure changes in the level of expression of known STAT5-regulated genes, including *MCL-1*, *C-MYC*, *cyclin D1*, and *cyclin D2*, in K562 cells. In keeping with our hypothesis, after treatment with 40 μM of **BP-1-108**, **BP-1-075**, **BP-1-111**, and **SF-1-087** for 6 h, we observed a significant reduction of *MCL-1*, *C-MYC*, *cyclin D1*, and *cyclin D2* mRNA (Figure 5). These data, in conjunction with the Western blot analysis of STAT5 phosphorylation, the potent *in vitro* disruption of STAT5/phosphopeptide complexation (Table 1), and whole cell results (Table 2), indicate that the lead STAT5 binding agents potently inhibit the transcriptional function of STAT5 and as a result suppress tumor cell growth, proliferation, and survival, culminating in cellular apoptosis.

To confirm that **BP-1-108** disrupted STAT5 binding to the *C-MYC* and *cyclin D1* promoter regions, we performed a chromatin immunoprecipitation assay (Millipore, Billerica, MA, USA). PCR of STAT5 immunoprecipitated chromatin fragments of whole cell lysates taken from K562 cells treated with **BP-1-108** (40 μM, 6 h) showed no STAT5 binding to either the *C-MYC* or *cyclin D1* promoter regions (Figure 6A) as compared with untreated control cells, in which pSTAT5 antibody was able to precipitate both *C-MYC* and *cyclin D1*

dx.doi.org/10.1021/jm200720n | J. Med. Chem. 2012, 55, 1047−1055

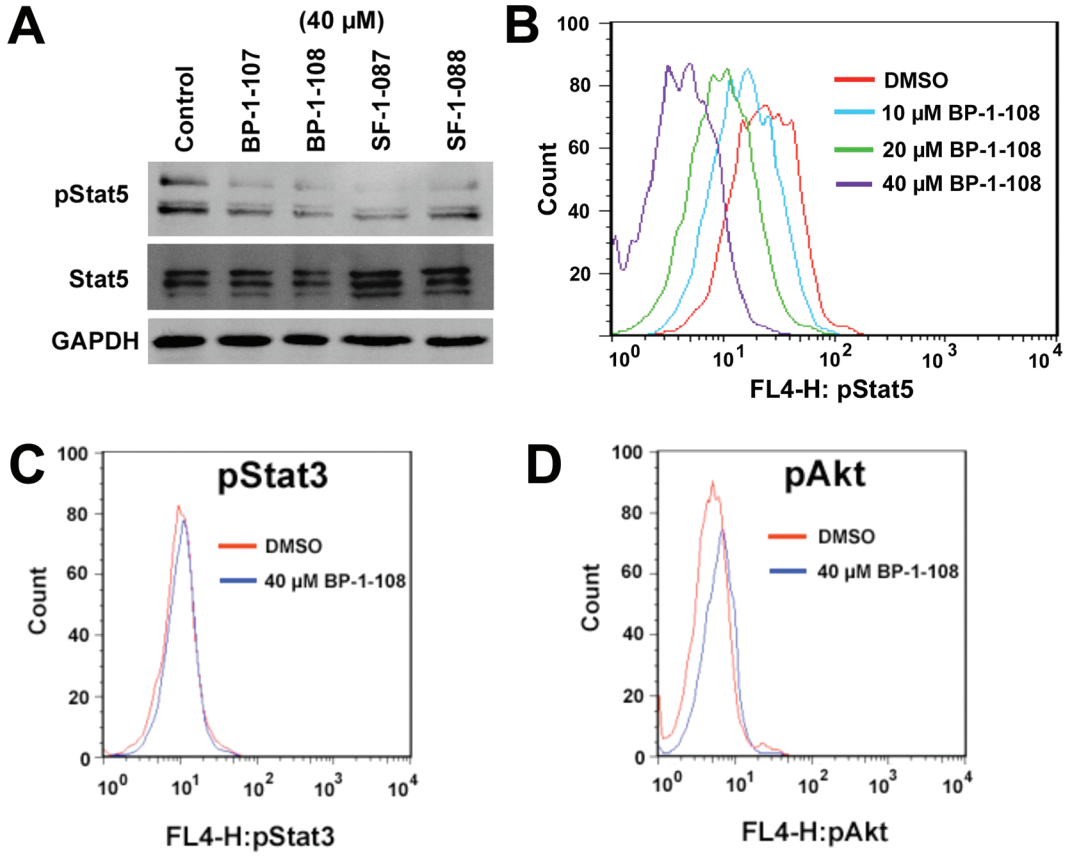

Figure 2. (A) Western blot analysis of STAT5 inhibition in K562 cells treated with **BP-1-107**, **BP-1-108**, **SF-1-087**, and **SF-1-088** STAT5 inhibitors. The different sized bands in the pSTAT5 and STAT5 panels arise due to alternate forms (STAT5a and STAT5b) and post-translational modifications of the proteins.[24,25] (B) Dose-dependent inhibition of pSTAT5 by **BP-1-108** as measured by phospho-flow cytometry. (C) Minimal inhibition of pSTAT3. (D) pAkt by **BP-1-108** as measured by phospho-flow cytometry.

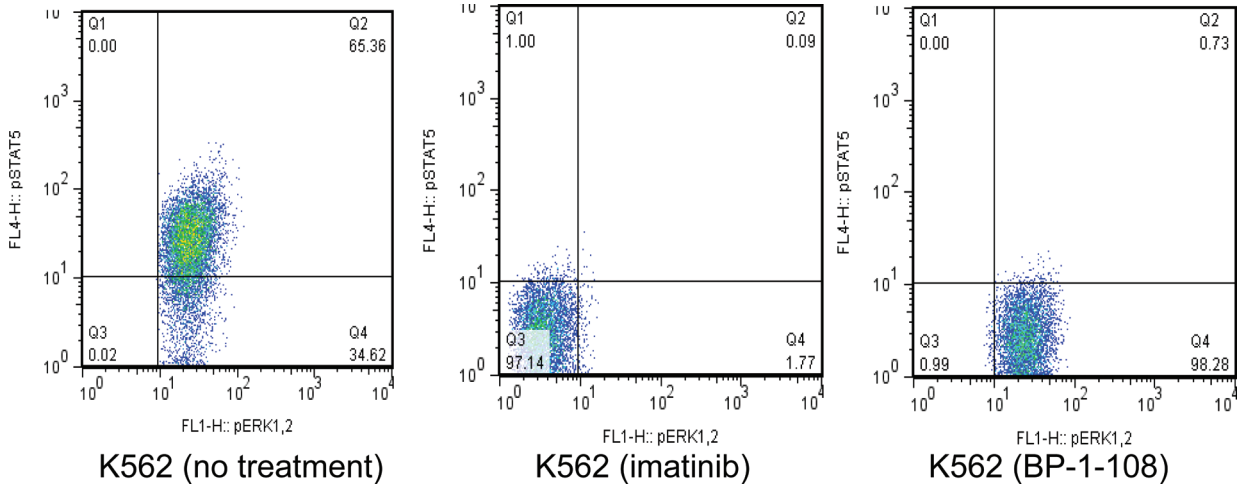

Figure 3. K562 cells nontreated or treated with imatinib or **BP-1-108** were fixed and stained for the levels of pSTAT5 and pERK1,2. The *Y* axis is pSTAT5, and the *X* axis is pERK1,2.

promoters (Figure 6B). Thus, **BP-1-108**-mediated inhibition of STAT5 activation can inhibit the high level expression of C-MYC and cyclin D1 in K562 leukemia cells.

■ CONCLUSIONS

In summary, we have identified a number of promising STAT5 SH2 domain inhibitors that exhibit potent and selective *in vitro* binding activity for STAT5, effectively disrupting STAT5/phosphopeptide interactions (K_i's < 5 μM). Moreover, unlike traditional SH2 domain targeting phosphopeptide mimetics, the structures identified do not contain a pharmacokinetically labile phosphotyrosyl group. Moreover, in AML cell lines MV-4-11, carrying a FLT3-ITD and BCR-ABL positive K562, our lead agent **BP-1-108** suppresses STAT5 phosphorylation and inhibits STAT5 mediated gene expression, including the down regulation of C-MYC, cyclin D1, cyclin D2, and MCL-1,

dx.doi.org/10.1021/jm200720n | *J. Med. Chem.* 2012, 55, 1047−1055

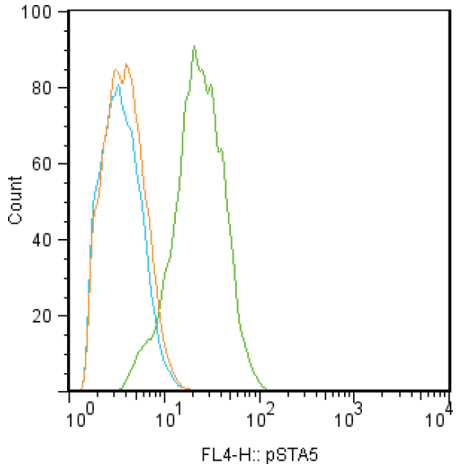

Figure 4. Effect of **BP-1-108** on IL-3 mediated phosphorylation of STAT5. IL-3 dependent 32D cells were assessed for the level of pSTAT5 by flow cytometry under different growth conditions; with IL-3 (green line), IL-3 and **BP-1-108** (blue line); or no IL-3 (orange line).

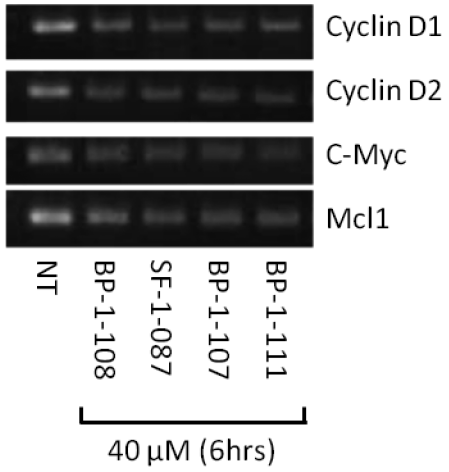

Figure 5. RT-PCR analysis of K562 whole cell lysates treated with **BP-1-108**, **BP-1−75, BP-1−111**, and **SF-1-087** to evaluate the levels of cMYC, Cyclin D1, Cyclin D2, and MCL-1 transcripts.

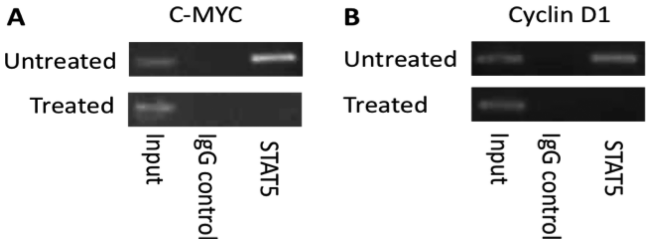

Figure 6. Chromatin immunoprecipitation of *C-MYC* and *cyclin D1* promoters using STAT5 antibody in K562 cells treated with 40 μM **BP-1-108**.

important inhibitors of apoptosis and regulators of the cell cycle. Particularly, MCL-1 has been shown as a key therapeutic target in leukemias.[24] As a result, **BP-1-108** exhibited encouraging antileukemic activity in K562 cells (IC_{50} = 17 μM) while showing no cytotoxicity against healthy bone marrow cells at concentrations up to 160 μM (Supporting Information). These molecules represent the most potent direct inhibitors of STAT5 function reported to date. Given the current dearth of small molecules effectively targeting STAT5−STAT5 protein complexes in human cancers, our work in conjunction with that of Berg[24] shows that STAT5 protein−protein interactions are an appealing and viable target for small molecule disruptors.

EXPERIMENTAL SECTION

Fluorescent Polarization Assay. Fluorescence polarization experiments were performed on an Infinite M1000 (Tecan, Crailsheim, Germany) using black 384-round-bottom well plates (Corning) and buffer containing 50 mM NaCl, 10 mM Hepes, pH 7.5, 1 mM EDTA, and 2 mM dithiothreitol and a final concentration of 5% DMSO. STAT protein (120 nM, 150 nM, and 105 nM for STAT1, STAT3, and STAT5, respectively) were treated with varying concentrations of inhibitor compounds (200 to 0.2 μM final concentrations). The fluorescent probe was added at a final concentration of 10 nM. Protein, inhibitor, and probe were combined and incubated for 15 min prior to analysis. Polarized fluorescence was plotted against concentration and fitted using a standard dose−response curve.

Cell Culture, Treatment, and Viability Testing. To determine whether STAT5 inhibitors could be cytotoxic in cell lines that have constitutive activation of STAT5, the cell lines K562 and MV-4-11 were cultured at a concentration of 1×10^5, to ensure that the cells are at the exponential stage of growth, and treated with the different synthesized molecules at concentrations of 10, 20, and 40 μM. Viability were determined using Almar Blue (Invitrogen) in a 96-well plate over 3 consecutive days. Fluorescence was quantified using Spectra Max M5 (Molecular Devices).

Annexin V/PI Assay. K562 cells treated with 40 μM of **BP-1-108** for 24 h or were untreated and washed twice with PBS and then stained consecutively with FITC-coupled Annexin V (Becton Dicknson) antibody for 15° and PI (Becton Dickinson) for 10°. Then, data were acquired using FacsCaliber and analyzed using FlowJo software.

Determining Inhibition of Intracellular STAT5, STAT3, and STAT1 Phosphorylation. Cells were treated with the potential STAT5 inhibitors for 6 h, then 1×10^7 were lysed using RIPA buffer. Lysates were loaded on SDS−PAGE in order to size-fractionate the proteins. Thereafter, proteins were blotted onto PVDF membrane (PALL Life Sciences). The membrane was blocked using 5% BSA in PBS containing 0.1% Tween 20 (Sigma) and then probed with antibodies against pSTAT5, STAT5, pSTAT3, STAT3 (Cell Signaling), and GAPDH. Secondary staining was performed with antirabbit IgG coupled with HRP (Amersham Bioecinces), and chemiluminescence reaction was carried out using ECL Plus (Amersham Biosciences). Proteins were quantified using Typhoon 9410 (Amersham Biosciences).

Inhibition of IL-3-Induced STAT5 Phosphorylation. IL-3 dependent 32D cells were grown in the absence of IL-3, with IL-3 alone, or with IL-3 and **BP-1-108** for 6 h. Following this, the cells were washed, fixed, stained for pSTAT5, and assessed by flow cytometry.

Flow Cytometry. K562 cells were treated (40 μM **BP-1-108**) or untreated for 6 h, then fixed and stained for pSTAT3, pSTAT5, pAKT1, or pERK1,2. For pSTAT3, pSTAT5 and pAKT1 nonlabeled rabbit monoclonal antibodies were used first, followed by detection with Cy5 coupled antirabbit IgG antibodies. pERK1 was detected using an Alexa448-coupled rabbit monoclonal antibody.

Chromatin Immunoprecipitation (ChIP). ChIP assay was performed using the EZ ChIP kit (Millipore, Billerica, MA, USA) as per the manufacturer's instructions. Briefly, after cross-linking with formaldehyde (1%), cells were lysed using SDS Lysis Buffer containing Protease Inhibitor Cocktail, and nuclear extracts were obtained. Then, cross-linked DNA was sheared using sonication; sheared DNA size was checked on agarose gel and ranged, in all cases, between 300 and 500 bp. An amount of 1/20 of the shared chromatin was kept as an input. Sheared chromatin was incubated with rabbit polyclonal Phospho-STAT5 (Tyr694) Antibody (Cell Signaling, Danvers, MA, USA) at a dilution of 1:50 or rabbit polyclonal IgG at an appropriate

dx.doi.org/10.1021/jm200720n | J. Med. Chem. 2012, 55, 1047−1055

concentration. Incubation was performed at 4 °C overnight. The antibody/chromatin complex was precipitated using Protein G Agarose beads. After elution, the cross-link of protein/DNA was reversed, and DNA was purified using Spin Columns. PCR was performed using platinum Taq (Invitrogen Canada, Burlington, ON, Canada). Two sets of primers were designed to amplify two DNA segments that contain STAT5-binding sites located 1672bp and 428bp upstream of the start sites of *C-MYC* and *cyclin D1*, respectively. The STAT5-binding site in the *C-MYC* promoter is characterized by a 4N spacer and has the sequence (ttcccccgaa), whereas the one in the *cylcin D1* promoter is characterized by a 3N spacer and has the sequence (ttcttggaa).

Chemical Methods. Anhydrous solvents methanol, DMSO, CH_2Cl_2, THF, and DMF were purchased from Sigma Aldrich and used directly from Sure-Seal bottles. Molecular sieves were activated by heating to 300 °C under vacuum overnight. All reactions were performed under an atmosphere of dry nitrogen in oven-dried glassware and were monitored for completeness by thin-layer chromatography (TLC) using silica gel (visualized by UV light or developed by treatment with $KMnO_4$ stain or phosphomolybdic acid stain). ^1H and ^{13}C NMR spectra were recorded on Bruker 400 MHz spectrometer in $CDCl_3$, CD_3OD, or d_6-DMSO. Chemical shifts (δ) are reported in parts per million after calibration to a residual isotopic solvent. Coupling constants (J) are reported in Hz. Before biological testing, inhibitor purity was evaluated by reversed-phase HPLC (rpHPLC). Analysis by rpHPLC was performed using a Microsorb-MV 300 A C18 250 mm × 4.6 mm column run at 1 mL/min and using gradient mixtures. The linear gradient consisted of a changing solvent composition of (I) 100% H_2O with 0.1% TFA for 2 min to 100% MeCN with 10% H_2O and 0.1% TFA (v/v) at 22 min and UV detection at 254 nm, (II) 100% H_2O with 0.1% TFA for 2 min to 100% MeCN with 10% H_2O and 0.1% TFA (v/v) at 62 min and UV detection at 214 nm, (III) 100% H_2O (0.01 M NH_4OAc) for 2 min to 100% MeOH at 22 min and UV detection at 254 nm or (IV) 100% H_2O (0.01 M NH_4OAc) for 2 min to 100% MeOH at 62 min and UV detection at 254 nm, (V) 100% H_2O (0.01 M NH_4OAc) for 2 min to 100% MeOH at 25 min and UV detection at 254 nm, or (VI) 100% H_2O (0.01 M NH_4OAc) for 2 min to 100% MeOH at 62 min and UV detection at 254 nm, each ending with 5 min of 100% B. For reporting HPLC data, percentage purity is given in parentheses after the retention time for each condition. All biologically evaluated compounds are >95% chemical purity as measured by HPLC. The HPLC traces for all tested compounds are provided in Supporting Information.

Final Molecule Characterization. ***(SF1-066)*** *4-(N-(4-Cyclohexylbenzyl)-2-(N,4-dimethylphenylsulfonamido)acetamido)-2-hydroxybenzoic Acid.* δ_H (400 MHz, d_6-DMSO) 1.14−1.40 (m, 5H, CH_2), 1.64 − 1.81 (m, 5H, CH_2), 2.36 (s, 3H, CH_3Ar), 2.44 (s (br), 1H, CH), 2.77 (s, 3H, NCH_3), 3.86 (s, 2H, $COCH_2$), 4.79 (s, 2H, CH_2Ar), 6.79 (d, J = 8.6 Hz, 1H, CH (Ar)), 6.86 (s (br), 1H, CH (Ar)), 7.06 (d, J = 7.8 Hz, 2H, 2 CH (Ar)), 7.13 (d, J = 7.8 Hz, 2H, 2 CH (Ar)), 7.35 (d, J = 8.0 Hz, 2H, 2 CH (Ar)), 7.54 (d, J = 8.0 Hz, 2H, 2 CH (Ar)), 7.77 (d, J = 8.3 Hz, 1H, CH (Ar)), 11.30 (s (br), 1H, OH); δ_C (400 MHz, d_6-DMSO) 21.2, 25.1(2), 26.6, 34.2, 36.1, 42.3, 43.6, 51.2, 51.9, 112.7, 116.3, 118.9, 126.9, 127.2, 127.8, 129.9, 131.6, 134.5, 135.3, 143.4, 146.8, 147.3, 161.8, 167.0, 171.5; HRMS (ES+) calcd for $[C_{30}H_{35}N_2O_6S + H]$ 551.2223; found, 551.2210; HPLC (I) t_R = 24.35 min (98.11%), (II) t_R = 52.80 min (98.16%).

(BP1-075) *4-(2-(N,4-Dimethylphenylsulfonamido)-N-((3′-(methoxycarbonyl)terphenyl-4-yl)methyl) acetamido)-2-hydroxybenzoic Acid.* δ_H (400 MHz, d_6-DMSO) 2.36 (s, 3H, CH_3), 2.81 (s, 3H, CH_3), 4.90 (s, 2H, CH_2), 6.80 (d, 1H, J = 8.4 Hz, CH), 6.89 (s, 1H, CH), 7.29 (d, J = 8.4 Hz, 2H, CH), 7.36 (d, J = 8.0 Hz, 2H, CH), 7.61−7.67 (m, 5H, CH), 7.76−7.79 (m, 4H, CH), 7.96 (d, J = 7.6 Hz, 1H, CH), 8.00 (d, J = 8.0 Hz, 1H, CH), 8.24 (s, 1H, CH), 8.32 (s, 1H, CH); δ_C (400 MHz, d-$CDCl_3$) 20.87, 35.80, 50.85, 51.57, 52.16, 115.95, 117.44, 118.14, 126.47, 126.89, 127.13, 127.20, 127.34, 127.89, 128.05, 128.34, 129.46, 129.54, 130.30, 131.26, 135.06, 136.38, 137.86, 138.17, 139.10, 139.98, 143.05, 146.39, 161.85, 166.04, 166.73, 171.05; HRMS (ES+) calcd for $[C_{37}H_{32}N_2O_8S + H]$ 679.2108; found, 679.2080; HPLC (I) t_R = 23.34 min (96.76%), (II) t_R = 50.50 min (98.76%).

(BP2-122) *4-(N-((4″-Carbamoyl-[1,1′:4′,1″-terphenyl]-4-yl)-methyl)-2-(N,4-dimethylphenyl sulfonamido)acetamido)-2-hydroxybenzoic Acid.* δ_H (400 MHz, d_6-DMSO) 2.35 (s, 3H, CH_3), 2.79 (s, 3H, CH_3), 3.87 (s, 2H, CH2), 4.88 (s, 2H, CH_2), 6.78 (d, J = 6.4 Hz, 1H, CH), 6.86 (s, 1H, CH), 7.29 (d, J = 8.4 Hz, 2H, CH), 7.37 (d, J = 8.0 Hz, 2H, CH), 7.55−7.69 (m, 6H, CH), 7.76−7.84 (m, 4H, CH), 7.95−8.04 (m, 3H, CH); δ_C (100 MHz, d_6-DMSO) 21.3, 30.7, 51.3, 52.0, 103.0, 116.2, 118.4, 126.2, 126.5, 127.0, 127.1, 127.3, 128.2, 128.4, 128.7, 128.8, 129.6, 131.4, 131.5, 132.0, 132.1, 132.2, 133.1, 133.2, 135.1, 136.4, 138.1, 138.3, 139.1, 142.1, 143.1, 146.8, 161.7, 166.8, 167.5, 171.1, 172.0; HRMS (ES+) calcd for $[C_{37}H_{33}N_3O_7S + H]$ 664.2111; found, 664.2141; HPLC (III) t_R = 19.22 min (76.63%), (IV) t_R = 43.81 min (79.95%).

(SF2-096) *4-(N-(4-(1-(4-Cyanophenyl)piperidin-4-yl)benzyl)-2-(N,4-dimethylphenyl-sulfon-amido)acetamido)-2-hydroxybenzoic Acid.* δ_H (400 MHz, d_6-DMSO) 1.56−1.68 (m, 2H, CH_2), 1.80−1.83 (m, 2H, CH_2), 2.36 (s, 3H, CH_3), 2.74−2.75 (m, 1H, CH), 2.52−2.53 (m, 2H, CH_2), 2.77 (s, 3H, CH_3), 2.88−2.98 (m, 2H, CH2), 3.86 (s, 2H, CH_2), 4.80 (s, 2H, CH_2), 6.79 (dd, J = 8.0 and 2.0 Hz, 1H, CH), 6.87 (d, J = 2.0 Hz, 1H, CH), 7.03 (d, J = 7.2 Hz, 2H, CH), 7.09 (d, J = 8.0 Hz, 2H, CH), 7.17 (d, J = 8.0 Hz, 2H, CH), 7.35 (d, J = 8.0 Hz, 2H, CH), 7.53−7.56 (m, 4H, CH), 7.77 (d, J = 8.4 Hz, 1H, CH); δ_C (100 MHz, d-$CDCl_3$) 21.4, 29.5, 32.4, 35.8, 41.9, 48.2, 51.5, 52.9, 99.4, 114.3, 116.8, 118.9, 126.8, 127.4, 128.6, 129.4, 133.4, 134.3, 134.9, 143.4, 144.8, 147.4, 153.2, 162.8, 165.6, 171.8; LRMS (ES+) calcd for $[C_{36}H_{36}N_4O_6S + H]$ 653.24; found, 653.46 [M + H]; HPLC (I) t_R = 23.32 min (99.22%), (II) t_R = 49.33 min (99.66%).

(SF3-006) *4-(N-(4-(1-(4-Carbamoylphenyl)piperidin-4-yl)benzyl)-2-(N,4-dimethyl-phenyl-sulfonamido)acetamido)-2-hydroxybenzoic acid.* δ_H (400 MHz, d_6-DMSO) 1.66−1.80 (m, 2H, CH_2), 1.82−1.91 (m, 2H, CH_2), 2.33 (s, 3H, CH_3), 2.58−2.68 (m, 1H, CH), 2.77 (s, 3H, CH_3), 2.86 (t, J = 12.0 Hz, 2H, CH_2), 3.72 (s, 2H, CH_2), 3.89 (d, J = 12.0 Hz, 2H, CH_2), 4.75 (s, 2H, CH_2), 6.49 (d, J = 7.2 Hz, 1H, CH), 6.58 (s, 1H, CH), 6.87 (d, J = 8.8 Hz, 2H, CH), 7.00−7.09 (m, 4H, CH), 7.20 (d, J = 8.0 Hz, 1H, CH), 7.54 (d, J = 8.0 Hz, 1H, CH), 7.67 (d, J = 8.4 Hz, 2H, CH), 7.80 (d, J = 8.0 Hz, 1H, CH); δ_C (100 MHz, d_6-DMSO) 21.2, 29.4, 32.5, 35.7, 41.9, 51.3, 52.7, 114.1, 116.4, 118.6, 121.6, 126.7, 127.2, 128.5, 128.9, 129.4, 132.0, 134.2, 134.9, 143.4, 144.9, 146.5, 150.2, 153.6, 162.4, 166.8, 169.2, 171.3; HRMS (ES+) calcd for $[C_{36}H_{38}N_4O_7S + H]$ 671.2533; found, 671.2545; HPLC (III) t_R = 17.72 min (84.23%), (IV) t_R = 24.81 min (74.07%).

(BP1-107) *4-(N-(4-Cyclohexylbenzyl)-2-(N-methylbiphenyl-4-ylsulfonamido)acetamido)-2-hydroxybenzoic Acid.* δ_H (400 MHz, d_6-DMSO) 1.23−1.38 (m, 5H, CH_2), 1.62−1.78 (m, 5H, CH_2), 2.35−2.44 (m, 1H, CH), 2.08 (s, 3H, CH_3), 3.96 (s, 2H, CH_2), 4.78 (s, 2H, CH_2), 6.80 (dd, J = 8.4 and 2.0 Hz, 1H, CH), 6.89 (d, J = 2.0 Hz, 1H, CH), 7.04 (d, J = 8.0 Hz, 2H, CH), 7.09 (d, J = 8.4 Hz, 2H, CH), 7.44 (d, J = 8.0 Hz, 1H, CH), 7.51 (t, J = 7.6 Hz, 2H, CH), 7.68−7.81 (m, 5H, CH), 7.86 (d, J = 8.4 Hz, 2H, CH); δ_C (100 MHz, d_6-DMSO) 25.4, 26.2, 33.7, 35.8, 43.2, 50.7, 51.6, 115.9, 118.4, 120.3, 126.5, 126.9, 127.2, 127.4, 127.5, 128.4, 129.0, 131.3, 134.1, 136.9, 138.3, 144.1, 146.3, 146.8, 161.6, 166.5, 171.1; HRMS (ES+) calcd for $[C_{35}H_{36}N_2O_6S + H]$ 613.2366; found, 613.2356; HPLC (V) t_R = 22.09 min (96.50%), (VI) t_R = 38.47 min (89.47%).

(BP1-108) *4-(N-(4-Cyclohexylbenzyl)-2-(N,2,4,6-tetramethylphenylsulfonamido)acetamido)-2-hydroxybenzoic Acid.* δ_H (400 MHz, d_6-DMSO) 1.26−1.40 (m, 5H, CH_2), 1.64−1.81 (m, 5H, CH_2), 2.26 (s, 3H, CH_3), 2.44 (s, 7H, CH_3 and CH), 2.84 (s, 3H, CH_3), 3.84 (s, 2H, CH_2), 4.75 (s, 2H, CH_2), 6.62 (dd, J = 8.4 and 2.0 Hz, 1H, CH), 6.70 (d, J = 2.0 Hz, 1H, CH), 6.99 (d, J = 8.0 Hz, 2H, CH), 7.03 (s, 2H, CH), 7.11 (d, J = 8.0 Hz, 2H, CH), 7.75 (d, J = 8.4 Hz, 1H, CH); δ_C (100 MHz, d_6-DMSO) 20.3, 22.1, 25.4, 26.2, 33.8, 34.4, 43.2, 49.1, 51.5, 116.0, 118.4, 120.2, 126.5, 127.4, 131.2, 131.7, 132.1, 134.1, 139.4, 142.1, 146.7, 146.7, 161.5, 166.6, 171.0; HRMS (ES+) calcd for $[C_{32}H_{38}N_2O_6S + H]$ 613.2366; found, 613.2356; HPLC (V) t_R = 21.29 min (96.82%), (VI) t_R = 37.54 min (95.30%).

(BP1-111) *4-(2-(4-Chloro-N-methylphenylsulfonamido)-N-(4-cyclohexylbenzyl)acetamido)-2-hydroxybenzoic Acid.* δ_H (400

MHz, *d*-$CDCl_3$) 1.34 (m, 5H, CH_2), 1.75 (m, 5H, CH_2), 2.44 (m, 1H, CH), 2.84 (s, 3H, CH_3), 3.96 (s, 2H, CH_2), 4.77 (s, 2H, CH_2), 6.80 (dd, J = 8.4 and 2.0 Hz, 1H, CH), 6.89 (d, J = 2.0 Hz, 1H, CH), 7.04 (d, J = 8.0 Hz, 2H, CH), 7.13 (d, J = 8.0 Hz, 2H, CH), 7.64 (d, J = 8.8 Hz, 2H, CH), 7.72 (d, J = 8.8 Hz, 2H, CH), 7.78 (d, J = 8.4 Hz, 1H, CH); δ_C (100 MHz, *d*-$CDCl_3$) 25.4, 26.2, 33.8, 35.8, 43.2, 50.8, 51.6, 112.4, 115.9, 118.4, 126.5, 127.4, 128.8, 129.1, 131.2, 134.1, 137.1, 137.5, 146.4, 146.8, 161.5, 166.4, 171.0; HRMS (ES+) calcd for $[C_{29}H_{31}ClN_2O_6S$ +H] 571.1664; found, 571.1682; HPLC (V) t_R = 20.92 min (96.73%), (VI) t_R = 35.97 min (97.88%).

*(**SF1-087**) 4-(2-(N-(tert-Butoxycarbonyl)-4-methylphenylsulfonamido)-N-(4-cyclohexyl benzyl)acetamido)-2-hydroxybenzoic Acid.* δ_H (400 MHz, $CDCl_3$) 1.22−1.45 (m, 14H), 1.70−1.85 (m, 5H, CH_2), 2.42 (s, 3H, CH_3), 2.46 (s (br), 1H, CH), 4.46 (s, 2H, $COCH_2$), 4.91 (s, 2H, CH_2Ar), 6.70 (d, J = 8.0 Hz, 1H, CH (Ar)), 6.82 (s (br), 1H, CH (Ar)), 7.10−7.15 (m, 4H, 4 CH (Ar)), 7.30 (d, J = 8.0 Hz, 2H, 2 CH (Ar)), 7.88 (d, J = 8.4 Hz, 1H, 1 CH (Ar)), 8.02 (d, J = 8.2 Hz, 2H, 2 CH (Ar)), 10.66 (s (br), 1H, OH); !C (100 MHz, $CDCl_3$) 21.6, 26.0, 26.8, 27.7, 34.3, 44.2, 47.5, 53.1, 84.7, 111.6, 117.2, 119.3, 126.9, 128.3, 128.8, 129.0, 132.3, 133.5, 136.6, 144.2, 147.5, 147.9, 50.5, 162.9, 166.7, 172.6; HRMS (ES+) calcd for $[C_{34}H_{41}N_2O_8S$ + H] 637.2547; found, 637.2578; HPLC (I) t_R = 26.55 min (97.80%), (II) t_R = 59.27 min (100%).

*(**SF1-088**) 4-(N-Benzyl-2-(N-(tert-butoxycarbonyl)-4-methylphenylsulfonamido)acetamido)-2-hydroxybenzoic Acid.* δ_H (400 MHz, $CDCl_3$) 1.31 (s, 9H, 3(CH_3)), 2.41 (s, 3H, CH_3Ar), 4.47 (s, 2H, $COCH_2$), 4.95 (s, 2H, CH_2Ar), 6.69 (d, J = 8.4 Hz, 1H, CH (Ar)), 6.81 (s, 1H, CH (Ar)), 7.20−7.32 (m, 7H, CH (Ar)), 7.87 (d, J = 8.4 Hz, 1H, CH (Ar)), 8.00 (d, J = 8.2 Hz, 2H, 2 CH (Ar)), 10.68 (s (br), 1H, OH); δ_C (400 MHz, $CDCl_3$) 21.6, 27.7, 47.4, 53.3, 84.8, 111.6, 117.2, 119.2, 127.7, 128.4, 128.5, 128.7, 129.0, 132.3, 136.2, 136.6, 144.2, 147.7, 150.6, 162.9, 166.8, 172.6; HRMS (ES+) calcd for $[C_{28}H_{31}N_2O_8S$ + H] 557.1615; found, 577.1615; HPLC (I) t_R = 21.67 min (99.02%), (II) t_R = 46.05 min (98.14%).

■ ASSOCIATED CONTENT

Ⓢ Supporting Information

Chemical methods; selected FP binding data; cell culture, treatment and viability testing; annexin V/PI assay; determining the inhibition of intracellular Stat5, Stat3, and Stat1 phosphorylation; real-time RT-CR; chromatin immunoprecipitation (ChIP); effect of BP-1-108 on Stat5 by electrophoretic mobility shift assay (EMSA); sequences of primers used in quantitative real-time RT-PCR; and sequences of primers used in promoter regions amplification post ChIP. This material is available free of charge via the Internet at http://pubs.acs.org.

■ AUTHOR INFORMATION

Corresponding Author

*Department of Chemical and Physical Sciences, University of Toronto, Mississauga, 3359 Mississauga Road North, Mississauga, ON, L5L 1C6 Canada. Tel: 905-828-5354. Fax: 905-569-5425. E-mail: patrick.gunning@utoronto.ca.

Author Contributions

‖These authors contributed equally to this work.

■ ACKNOWLEDGMENTS

This work was supported by the National Science Engineering Research Councils (NSERC) (to P.T.G.), University of Toronto (to P.T.G.), Leukemia and Lymphoma Society of Canada (to M.M.), and an NSERC training fellowship (to B.D.G.P.).

■ REFERENCES

(1) Lai, S. Y.; Johnson, F. M. Defining the role of the JAK-STAT pathway in head and neck and thoracic malignancies: Implications for future therapeutic approaches. *Drug Resist. Updates* **2010**, *13*, 67−78.

(2) Müller, J.; Sperl, B.; Reindl, W.; Kiessling, A.; Berg, T. Discovery of chromone-based inhibitors of the transcription factor STAT5. *ChemBioChem* **2008**, *9*, 723−727.

(3) Page, B. D.; Ball, D. P.; Gunning, P. T. Signal transducer and activator of transcription 3 inhibitors: A patent review. *Expert Opin. Ther. Pat.* **2011**, *21*, 65−83.

(4) Fletcher, S.; Drewry, J. A.; Shahani, V. M.; Page, B. D. G.; Gunning, P. T. Molecular disruption of oncogenic signal transducer and activator of transcription 3 (STAT3) protein. *Biochem. Cell Biol.* **2009**, *87*, 825−833.

(5) Haftchenary, S.; Avadisian, M.; Gunning, P. T. Inhibiting aberrant Stat3 function with molecular therapeutics: A progress report. *Anticancer Drugs* **2011**, *22*, 115−127.

(6) Neculai, D.; Neculai, A. M.; Verrier, S.; Straub, K.; Klumpp, K.; Pfitzner, E.; Becker, S. Structure of the unphosphorylated STAT5a dimer. *J. Biol. Chem.* **2005**, *280*, 40782−40787.

(7) Tan, S. H.; Nevalainen, M. T. Signal transducer and activator of transcription 5A/B in prostate and breast cancers. *Endocr. Relat. Cancer* **2008**, *15*, 367−390.

(8) Ferbeyre, G.; Moriggl, R. The role of Stat5 transcription factors as tumor suppressors or oncogenes. *Biochim. Biophys. Acta* **2011**, *1815*, 104−114.

(9) Gouilleux-Gruart, V.; Debierre-Grockiego, F.; Gouilleux, F.; Capiod, J. C.; Claisse, J. F.; Delobel, J.; Prin, L. Activated Stat related transcription factors in acute leukemia. *Leuk. Lymphoma* **1997**, *28*, 83−88.

(10) Gouilleux-Gruart, V.; Gouilleux, F.; Desaint, C.; Claisse, J. C.; Capiod, J. F.; Delobel, J.; Weber-Nordt, R.; Dusanter-Fourt, I.; Dreyfus, F.; Groner, B.; Prin, L. STAT-related transcription factors are constitutively activated in peripheral blood cells from acute leukemia patients. *Blood* **1996**, *87*, 1692−1697.

(11) Weber-Nordt, R. M.; Egen, C.; Wehinger, J.; Ludwig, W.; Gouilleux-Gruart, V.; Mertelsmann, R.; Finke, J. Constitutive activation of STAT proteins in primary lymphoid and myeloid leukemia cells and in Epstein-Barr virus (EBV)-related lymphoma cell lines. *Blood* **1996**, *88*, 809−816.

(12) Pardanani, A.; Vannucchi, A. M.; Passamonti, F.; Cervantes, F.; Barbui, T.; Tefferi, A. JAK inhibitor therapy for myelofibrosis: Critical assessment of value and limitations. *Leukemia* **2011**, *25*, 218−225.

(13) Quintás-Cardama, A.; Kantarjian, H.; Cortes, J.; Verstovsek, S. Janus kinase inhibitors for the treatment of myeloproliferative neoplasias and beyond. *Nature Rev. Drug Discovery* **2011**, *10*, 127−140.

(14) Muller, J.; Schust, J.; Berg, T. A high-throughput assay for signal transducer and activator of transcription 5b based on fluorescence polarization. *Anal. Biochem.* **2008**, *375*, 249−254.

(15) Siddiquee, K.; Zhang, S.; Guida, W. C.; Blaskovich, M. A.; Greedy, B.; Lawrence, H. R.; Yip, M. L. R.; Jove, R.; McLaughlin, M. M.; Lawrence, N. J.; Sebti, S. M.; Turkson, J. Selective chemical probe inhibitor of Stat3, identified through structure-based virtual screening, induces antitumor activity. *Proc. Natl. Acad. Sci. U.S.A.* **2007**, *104*, 7391−7396.

(16) Fletcher, S.; Singh, J.; Zhang, X.; Yue, P.; Page, B. D. G.; Sharmeen, S.; Shahani, V. M.; Zhao, W.; Schimmer, A. D.; Turkson, J.; Gunning, P. T. Disruption of transcriptionally active stat3 dimers with non-phosphorylated, salicylic acid-based small molecules: Potent in vitro and tumor cell activities. *ChemBioChem* **2009**, *10*, 1959−1964.

(17) Zhang, X.; Yue, P.; Fletcher, S.; Zhao, W.; Gunning, P. T.; Turkson, J. A novel small-molecule disrupts Stat3 SH2 domain-phosphotyrosine interactions and Stat3-dependent tumor processes. *Biochem. Pharmacol.* **2010**, *79*, 1398−1409.

(18) Wu, P.; Brasseur, M.; Schindler, U. A high-throughput STAT binding assay using fluorescence polarization. *Anal. Biochem.* **1997**, *249*, 29−36.

(19) Schust, J.; Berg, T. A high-throughput fluorescence polarization assay for signal transducer and activator of transcription 3. *Anal. Biochem.* **2004**, *330*, 114−118.
(20) Bromberg, J. Stat proteins and oncogenesis. *J. Clin. Invest.* **2002**, *109*, 1139−1142.
(21) Jones, G.; Willett, P.; Glen, R. C.; Leach, A. R.; Taylor, R. Development and validation of a genetic algorithm for flexible docking. *J. Mol. Biol.* **1997**, *267*, 727−748.
(22) Quentmeier, H.; Reinhardt, J.; Zaborski, M.; Drexler, H. G. FLT3 mutations in acute myeloid leukemia cell lines. *Leukemia* **2003**, *17*, 120−124.
(23) De Groot, R. P.; Raaijmakers, J. A. M.; Lammers, J. -. J.; Jove, R.; Koenderman, L. STAT5 activation by Bcr-Abl contributes to transformation of K562 leukemia cells. *Blood* **1999**, *94*, 1108−1112.
(24) Meinke, A.; Barahmand-Pour, F.; Wohrl, S.; Stoiber, D.; Decker, T. Activation of different Stat5 isoforms contributes to cell-type-restricted signaling in response to interferons. *Mol. Cell. Biol.* **1996**, *16*, 6937−6944.
(25) Atsushi, O.; Hiroshi, W.; Fujita, H. Calpain is a signal transducer and activator of transcription (STAT)3 and Stat5 protease. *Blood* **2002**, *99*, 1850−1852.
(26) Yoshimoto, G.; Miyamoto, T.; Jabbarzadeh-Tabrizi, S.; Iino, T.; Rocnik, J. L.; Kikushige, Y.; Mori, Y.; Shima, T.; Iwasaki, H.; Takenaka, K.; Nagafuji, K.; Mizuno, S.; Niiro, H.; Gilliland, G. D.; Akashi, K. FLT3-ITD up-regulates MCL-1 to promote survival of stem cells in acute myeloid leukemia via FLT3-ITD-specific STAT5 activation. *Blood* **2009**, *114*, 5034−5043.